J. Phys. B: At. Mol. Opt. Phys. **29** (1996) 3747–3761. Printed in the UK

R-matrix calculation of the bound and continuum states of the e^-–NO^+ system

I Rabadán and J Tennyson†

Department of Physics and Astronomy, University College London, Gower Street, London WC1E 6BT, UK

Received 4 April 1996

Abstract. A comprehensive theoretical study of NO Rydberg states and of Feshbach resonances associated with excited states of NO^+ is made for an internuclear separation of 2.175 a_0. Calculations are performed using the UK *R*-matrix molecular package. The lowest four target states (X $^1\Sigma^+$, a $^3\Sigma^+$, b $^3\Pi$ and w $^3\Delta$) are considered in the construction of the CI target wavefunction. Quantum defect theory is employed to analyse the multiple Rydberg series obtained. In the bound-states region of the NO spectrum, six Rydberg series are resolved and quantum defects are given up to $n = 11$. In the continuum spectrum, Rydberg series of resonances converging to the three excited states of NO^+ considered are identified and compared with available experimental data. Some previous assignments for both bound and continuum states are reinterpreted and the dominant source of partial-wave mixing re-analysed. Data for the resonance widths are presented for the first time.

1. Introduction

NO^+ is one of the most important molecular ions in the E region of the ionosphere (100–150 km) and is also present in the F region (above 150 km) (Wayne 1991). Its main source is the photoionization of NO by EUV radiation from the Sun that takes place in the D region (60–100 km). The high electron density in these layers of the atmosphere makes the study of the collisional system e^-–NO^+ very important. One of the most important processes to study in this system is that leading to dissociative recombination ($NO^+ + e \rightarrow N + O$).

The theoretical study both of the ionization of NO and of dissociative recombination of NO^+ requires good wavefunctions for the continuum of the $e^- - NO^+$ system. To obtain these wavefunctions, we use the molecular *R*-matrix method (UK *R*-matrix package, see Gillan *et al* 1995), whose usefulness in similar studies has been shown previously (Tennyson *et al* 1984, Tennyson 1988). Once *R*-matrix wavefunctions for the system are obtained, they can also be used to study the bound Rydberg states of the system (Sarpal *et al* 1991). Thus, we can study, using the same theoretical description, the NO spectrum from its low-lying Rydberg states up to the high Feshbach or 'Rydberg' resonances converging to excited states of NO^+.

The spectrum of the NO molecule has been studied experimentally for the last seventy years (Huber and Herzberg 1979). Low-lying Rydberg states are well known (Miescher 1976). More recent experimental techniques such as ZEKE (Vrakking and Lee 1995) and double resonance spectroscopy (see, for example, Fujii *et al* 1990) have allowed the

† On sabbatical at: Institute for Theoretical Atomic and Molecular Physics, Harvard–Smithsonian Center for Astrophysics, 60 Garden Street, Cambridge, MA 02138, USA.

0953-4075/96/163747+15$19.50

study of high-lying Rydberg states ($n = 50$–100). Finally, experiments using time-of-flight photoelectron spectroscopy combined with two-colour double resonance (Park *et al* 1996) have provided a deep insight into the dynamics of the vibrational ionization of Rydberg states.

On the theoretical side, systematic studies of low-lying Rydberg states have been performed by Hermann *et al* (1986) and Kaufmann (1991). The information available makes NO a benchmark molecule and the first objective of this work is to make a comprehensive study of the NO Rydberg states. This both establishes the reliability of the R-matrix method for describing Rydberg states and extends the theoretical results available.

The continuum spectrum of the e^-–NO^+ system has been studied both theoretically (Hermann *et al* 1986, Stratmann *et al* 1996) and experimentally (Erman *et al* 1995, Guo *et al* 1995) through photoionization. However, we are not aware of either experiments or calculations from the collisional point of view. In particular, while there is a considerable amount of data available on low-lying resonance positions for this system, very little seems to be known about the corresponding widths.

Our second, but no less important, objective is to study the electron scattering from NO^+. This gives rise to a spectrum of resonances in collisions which are both electronically elastic and inelastic. The behaviour of such resonances is vital for modelling the atmospherically important process of dissociative recombination.

In this work, we consider four states of the target ion NO^+: $X\ ^1\Sigma^+$, $a\ ^3\Sigma^+$, $b\ ^3\Pi$ and $w\ ^3\Delta$, each of which is represented by a configuration-interaction (CI) wavefunction. To analyse the Rydberg series converging to these ion states, we use quantum defect theory (QDT) (Seaton 1983, Moores and Saraph 1983). QDT allows the parametrization of large numbers of states and resonances by an adimensional quantity, the quantum defect.

This paper is organized as follows. In section 2 we give details of the theoretical treatment: the model we use to describe the target NO^+ and the representation of the continuum. In section 3 we present the study of the NO Rydberg series and comparisons with available data. In section 4 we analyse cross sections for electronic excitation of NO^+ and present results for Rydberg resonances in the elastic and inelastic electron scattering processes. Finally, in section 5, we summarize the results.

2. Method

In the molecular R-matrix method (see Huo and Gianturco (1995) for a recent compilation of the theory and some applications), phase space is divided into two regions by a sphere centred at the target centre of mass and a radius a (which is 18 a_0 in our case). In the inner region, the wavefunction for the $(N+1)$-electron system can be expressed as

$$\Psi_k = \mathcal{A} \sum_{i,j} a_{i,j,k} \Phi_i(1, \ldots, N) F_{i,j}(N+1) + \sum_i b_{i,k} \chi_i(1, \ldots, N+1) \qquad (1)$$

where $\mathcal{A}$ is the antisymmetrization operator, Φ_i are N-electron target wavefunctions, $F_{i,j}$ are continuum orbitals and χ_i are two-centre L^2 functions constructed from the target occupied and virtual molecular orbitals.

In this work, the target wavefunctions Φ_i are configuration-interaction (CI) expansions of individual N-electron configurations. These, in turn, are obtained from an SCF calculation using a basis set of $(10\sigma, 6\pi, 1\delta, 1\phi)$ STOs (Billingsley 1975) centred on each nucleus.

We use 16 target molecular orbitals $(9\sigma, 5\pi, 1\delta, 1\phi)$ in the calculation. The first five σ MOs were obtained from an SCF calculation on the $NO^+(X\ ^1\Sigma^+)$ ground state; orbitals

6–9σ came from an SCF calculation on $NO^+(a\,^3\Sigma^+)$, and the remainder from an SCF calculation on $NO^+(A\,^1\Pi)$. To construct the CI wavefunction of NO^+, we keep MOs 1, 2 and 3σ as a frozen core and build configurations by allocating the remaining eight electrons among the complete active space (CAS) orbitals 4, 5, 6σ and 1, 2π.

The continuum orbitals, $F_{i,j}$, are numerical functions expressed as a truncated partial-wave expansion around the centre of mass and whose radial parts are generated as a numerical solution of an isotropic Coulomb potential. In this expansion, we retained six partial waves for every symmetry considered and those solutions of our model potential with an energy below 5 Ryd. This produces 73 σ, 69 π and 66 δ functions. These were Schmidt orthogonalized to the occupied and virtual molecular orbitals.

The functions χ_i are constructed from the target orbitals and hold both the projectile and target electrons. These functions are of two types: those where the scattering electron enters the target active space, which relaxes the enforced orthogonality between the target and continuum orbitals, and those where the scattering electron occupies the extra target virtual orbitals, which allow for high-ℓ effects near the nuclei.

We performed calculations using a number of models. Here, however, only results for two models will be presented: a two-state model that includes states $X\,^1\Sigma^+$ and $a\,^3\Sigma^+$ in the NO^+ target expansion, and a four-state model in which NO^+ states $b\,^3\Pi$ and $w\,^3\Delta$ are also included. Most results are presented for the four-state model and two-state results are included for comparison.

All calculations are carried out at the equilibrium distance of NO (2.175 a_0), appropriate for studying bound states of NO. In table 1, we give the number of configuration state functions (CSFs) employed in the description of each target state and the vertical excitation energies obtained. We compare with the experimental results of Albritton *et al* (1979) and the theoretical values of Partridge *et al* (1990). The difference between our results and experimental values of about 4% is satisfactory given the small number of CSFs employed in our CI expansions.

Table 1. Vertical energy excitations (in eV) for the first four states of NO^+ at 2.175 a_0 of bond length.

State	CSFs	This work	Expt[a]	Calc.[b]
$X\,^1\Sigma^+$	76	0.0	0.0	0.0
$a\,^3\Sigma^+$	70	6.73	6.47	6.94
$b\,^3\Pi$	126	7.00	6.92	7.07
$w\,^3\Delta$	67	7.97	7.56	8.29

[a] Albritton *et al* (1979).

[b] Partridge *et al* (1990); values obtained by using the experimental ionization energy of 9.62 eV to fix the energy of the $NO^+(X\,^1\Sigma^+)$ state at this geometry.

The absolute energy of the $X\,^1\Sigma^+$ state in our calculation is $-129.066\,562$ Hartree, which can be compared with -129.133 Hartree interpolated from Fehér and Martin's (1993) CASSCF calculation. Our wavefunction gives an NO^+ dipole moment of 0.211 au, compared to 0.154 au interpolated from the calculation of Fehér and Martin. Our calculated NO^+ diagonal and off-diagonal target dipoles and quadrupoles were used to provide the interaction potential in the outer region.

3. Bound states

3.1. Searching procedure

Once the wavefunction (1) has been constructed in the inner region, the R-matrix is computed on the boundary and propagated (Morgan 1984) until the wavefunction can be matched with exponential decreasing functions obtained from a Gailitis expansion (Noble and Nesbet 1984). We tested R-matrix propagation to distances in the range 25–80 a_0 and found no significant differences in the results. We therefore settled on a value of 40 a_0.

In this work we study bound states that correspond to Rydberg states of NO for three symmetries: $^2\Sigma^+$, $^2\Pi$ and $^2\Delta$. To study these states it is particularly appropriate to use quantum defect theory (Seaton 1983), since it permits an easy identification of each Rydberg series by means of the adimensional quantum defect. The energy of a Rydberg state can be expressed as a sum of the energy of the core ion (NO^+ $X\ ^1\Sigma^+$) and the energy of the Rydberg electron, ε (a hydrogen-like expression):

$$E_{nl\lambda} = E(\mathrm{NO}^+\ \mathrm{X}\ ^1\Sigma^+) + \varepsilon_{nl\lambda} \tag{2}$$

where

$$\varepsilon_{nl\lambda} = -\frac{Z^2}{v_{nl\lambda}^2} = -\frac{Z^2}{(n-\alpha_{nl\lambda})^2}\,. \tag{3}$$

Here, energies are in Ryd, Z is the charge number of the core ion, v is the effective quantum number, integer n is the principal quantum number and $\alpha_{nl\lambda}$ is the quantum defect of the Rydberg electron. The quantum defect accounts for the strong interaction, both Coulombic and non-Coulombic, that the Rydberg electron experiences when it penetrates into the core ion. This interaction depends on the probability of finding the Rydberg electron inside the ion core, which is related to its angular momentum (l) and, to a lesser extent, the projection of this momentum on the molecular axis (λ). These ideas were used by Lindholm (1970) to estimate the quantum defects for several small molecules.

To obtain the energy $E_{nl\lambda}$ of the bound states, we adapted the method described by Sarpal *et al* (1991). In this method, the eigenvalue problem is reduced to finding the roots of a determinant, $\boldsymbol{B}(E)$, that depends on the energy of the system. In the original procedure, the roots of a $\boldsymbol{B}(E)$ were found by searching a linear grid in the effective quantum number v, which is related to the energy of the system through equations (2) and (3). As the values of the quantum defect α tend to be concentrated around 0 (with possible negative values), we used a non-linear grid for which the distance between grid points is smaller in the vicinity of integer values of v. Thus, we can find eigenstates with a quantum defect of $\alpha = 0.001$ using a grid of only 30 points per unit of v. A linear grid would have required 1000.

The non-linear grid is obtained from the linear one by passing the values of v through the function

$$f = \frac{1}{2}\left(\frac{\gamma^{\gamma/2}(2x-1)}{(\gamma-1+(2x-1)^2)^{\gamma/2}} + 1\right) \tag{4}$$

where $x = v - \mathrm{int}(v)$ and the next v' to substitute into equation (3) is given by $v' = \mathrm{int}(v) + f$. This function is well known in the field of ion–atom collisions as a 'common translation factor' (Errea *et al* 1994). γ controls the non-linearity of the grid and takes values in the interval $(1, \infty)$; the closer to 1, the larger is the concentration of grid points around integer values of v. In this work we have used $\gamma = 1.12$.

3.2. Results

In table 2, we present our results of the quantum defects for the Rydberg series $l = 0, 1, 2, 3$ and states up to $n = 11$. Experimental results for comparison are also given at the bottom of the table. There is reasonable quantitative agreement between our calculations and the experiment. Interestingly, the experimental quantum defects are systematically ~ 0.06 higher than ours for all series. Of course this is a larger proportion of the d-wave quantum defects, giving rise to what appears to be worse agreement in this case.

Table 2. Quantum defects of the Rydberg series converging to $NO^+(X\ ^1\Sigma^+)$ obtained with the four-state model and experimental results (bottom of the table).

n	sσ	pσ	pπ	dσ	dπ	dδ	fσ	fπ	fδ
2			0.7504						
3	1.0447	0.6928	0.7135	−0.0615	−0.0508	0.0125			
4	1.1320	0.6599	0.6960	−0.0775	−0.0649	0.0232	0.0074	0.0054	0.0010
5	1.1392	0.6489	0.6930	−0.0841	−0.0707	0.0286	0.0086	0.0059	0.0013
6	1.1417	0.6440	0.6949	−0.0875	−0.0736	0.0319	0.0093	0.0063	0.0014
7	1.1429	0.6413	0.6989	−0.0894	−0.0753	0.0341	0.0098	0.0066	0.0016
8	1.1436	0.6397	0.7041	−0.0907	−0.0764	0.0356	0.0101	0.0067	0.0017
9	1.1441	0.6387	0.7097	−0.0915	−0.0771	0.0367	0.0103	0.0068	0.0017
10	1.1444	0.6380	0.7155	−0.0921	−0.0776	0.0375	0.0105	0.0069	0.0018
11	1.1446	0.6376	0.7211	−0.0925	−0.0780	0.0384	0.0106	0.0071	0.0018
3	1.10[a]	0.74[a]	0.78[a]	−0.022[a]	−0.024[a]	0.058[a]			
4	1.19[b]	0.70[a]	0.76[a]	−0.035[b]	−0.036[b]	0.071[b]			
5	1.20[b]	0.68[a]	0.75[a]						
6	1.20[b]			−0.043[b]	−0.045[b]	0.081[b]			
7	1.20[b]					0.085[b]			

[a] Miescher and Huber (1976).
[b] Fredin *et al* (1987).

There are two possible causes for this discrepancy. One is that our calculation included insufficient correlation–polarization effects and thus yields states that are not sufficiently bound and hence quantum defects that are too low. Alternatively, the experimental results implicitly include the effects of nuclear motion which are absent from our calculation. This omission could also have a systematic effect on the quantum defect. Both of these effects will be the subject of future work.

Low-lying states are more sensitive to valence-shell correlation effects and are thus harder to model with scattering calculations. In particular, our four-state model predicts energies for states $X\ ^2\Pi$, $A\ ^2\Sigma^+$ and $C\ ^2\Pi$ of -8.71, -3.56 and -2.60 eV with respect to the $NO^+(X\ ^1\Sigma^+)$ ground state. The corresponding experimental values are -9.6, -3.8 and -2.8 eV, respectively (Gilmore 1965). Thus it is just the NO ground state for which the difference is large.

To analyse the results presented in table 2, we use the fact that quantum defects are smooth functions of ε (Seaton 1983) and, in most cases, can be approximated by a linear relation of this energy (Edlén 1964, Kaufmann 1991):

$$\alpha_{nl\lambda} = b + a\varepsilon_{nl\lambda} \tag{5}$$

where a and b are characteristic of each Rydberg series. Parameter b is related to the position of the wavefunction nodes inside the core ion, and a to the penetration of the electron into the core ion, i.e. the amplitude of the wavefunction within the core (Jastrow 1948, Kaufmann 1991).

In figure 1 we show the Edlén plots of equation (5) for the pπ and pσ series. For the pπ series we include the results of our two models: four-state (□) and two-state (◇). The main difference between these models is the general shift of the curve to higher values of α. This difference is given by a shift in parameter b of equation (5). From the interpretation of b given above, the inclusion of two additional target states improves the representation of the Rydberg wavefunction inside the core ion, but does not significantly alter its penetration.

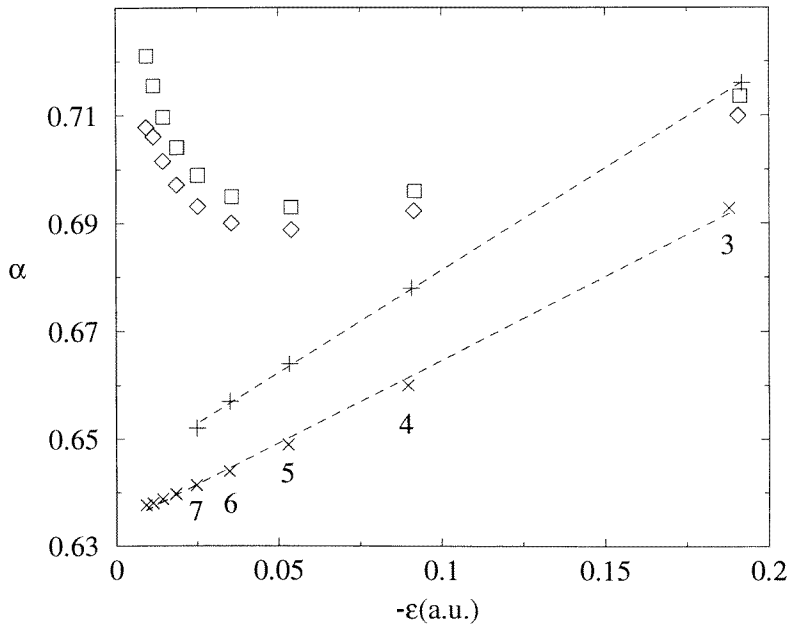

Figure 1. Edlén plot of the Rydberg series pσ and pπ of the NO molecule. For the pσ: ×, our results in the four-state model; +, CEPA results of Kaufmann (1991) for a bond length of 2.006 a_0; broken lines are least-square fits to the data. For the pπ series: □, four-state model; ◇, two-state model.

For the pσ series, figure 1 shows our four-state results (×) and the CEPA results of Kaufmann (1991) (+). In both cases, the broken line is a least-squares fit to the data and we note that this series closely follows the linear relation (5). The difference between results is mainly in the parameter b.

As we have seen with series pπ in figure 1, b is the main factor that changes when we go from the two- to the four-state model. Hence, the systematic deviation of our results from the observed ones seen in table 2 might be removed with a more complete close-coupling expansion of target states. Indeed we attempted an eight-target-state calculation but this proved intractable with the programs and computers used in the present work.

Only the pπ series is poorly approximated by the simple linear relationship, equation (5). Although one would not expect the NO(X $^2\Pi$) state to lie on the same line as the higher Rydberg states, the reason for the quadratic behaviour of this series is unclear. Table 3 presents the coefficients a and b obtained by means of a least-squares fit to equation (5) for all other Rydberg series. In this table, we compare results obtained using the four-state model and the reduced two-state model. The largest values in the parameters a and b, and the largest differences between the two models appear in the series s, p and d. Large a indicates that the series has a penetrating character, hence these series are sensitive to

improvements in the target expansion. This is especially true of the dδ series. The difference between models is smaller as the l character of the series increases. This is because high-l series are non-penetrating and thus less sensitive to the details of the target wavefunction.

Table 3. Coefficients of the quantum defect least-squares fit to equation (5).

	Four-state		Two-state			CEPA[a]	
Series	a	b	a	b	α_∞	a	b
sσ	−0.111	1.1459	−0.108	1.1455	1.150	−0.137	1.181
pσ	0.309	0.6338	0.316	0.6315	0.624	0.379	0.643
dσ	0.314	−0.0956	0.320	−0.0963	−0.103	0.327	−0.073
dπ	0.272	−0.0806	0.301	−0.0918	−0.099		
dδ	−0.247	0.0395	−0.202	0.0344	0.040		
fσ	−0.058	0.0100	−0.055	0.0108	0.020		
fπ	−0.031	0.0072	−0.030	0.0072	0.011		
fδ	−0.0158	0.0019	−0.0146	0.0018			
gσ	−0.0039	0.0027	−0.0038	0.0027			
gπ	−0.0028	0.0023	−0.0026	0.0023			
gδ	−0.0027	0.0012	−0.0028	0.0012			
hσ	−0.0013	0.0010	−0.0014	0.0010			
hπ	−0.0015	0.0012	−0.0015	0.0012			
hδ	−0.0015	0.0008	−0.0028	0.0008			

[a]Kaufmann (1991), results obtained for a bond length of 2.006 a_0.

Table 3 also compares our results with the theoretical CEPA results of Kaufmann (1991). The agreement is qualitatively good for both parameters a and b, although we note that Kaufmann's results are obtained for an NO^+ equilibrium bond length of 2.006 a_0.

Some of the older works on Rydberg states of NO show qualitatively different behaviour for the sσ and dσ series to that given above. In particular, we cite the theoretical works of Hermann *et al* (1986) and Lindholm (1970) and the experiments of Edqvist *et al* (1970). In these works, the slope a of the sσ series is positive and is negative in the dσ series. Furthermore, quantum defects are 0.95 for 4sσ and 0.16 for 4dσ. These quantum defects and behaviour are obtained if the states we assigned as nsσ are swapped with those taken to be ndσ.

One way to determine the l character of the different series is to look at the eigenvectors of the matrix $\boldsymbol{S}$ above threshold (Seaton 1983, Tennyson 1988). Calculations were performed at a scattering energy of 0.35 eV, and for a number of R-matrix propagation radii in an interval 150–250 a_0. Quantum defects obtained in this way within the two-state model are given in table 3 under the column α_∞. These results are in good agreement with the values given in column b, which are the extrapolation to $n = \infty$ obtained using equation (5) for values up to $n = 11$. Eigenvectors for these series show the following composition:

- sσ: 98% s, 1% p, 1% d
- pσ: 2% s, 57% p, 40% d
- dσ: 41% p, 58% d

confirming the assignments given here and by Kaufmann (1991).

These eigenvectors are surprising in view of the widely discussed and accepted s–d mixing of NO Rydberg states (see, for example, Kaufmann 1991, Liu and Li 1991, Fredin *et al* 1987, Miescher 1976). This mixing has been explained by the fact that NO is a quasi-homonuclear molecule and so the interaction s–p and p–d is forbidden by symmetry selection

rules. This argument would appear to be appropriate only for valence or low-n states. High-n states spend most of their time far from the nuclei. In this circumstance, dipole interactions will predominate over quadrupole ones. It should therefore not be surprising that large p–d mixing is obtained in the $n = \infty$ limit.

4. Continuum states

In this section we study the Rydberg resonances of NO converging to the excited states included in our four-state calculation. Rydberg states associated with the $NO^+(a\,^3\Sigma^+)$ state occur in the continuum spectrum of $NO^+(X\,^1\Sigma^+) + e^-$, and their possible manifestation is through resonances in the elastic scattering spectrum. Those associated with the $NO^+(b\,^3\Pi)$ state are embedded in two continua, the previous one and $NO^+(a\,^3\Sigma^+) + e^-$. They can be seen as resonances in the electronic excitation $NO^+(X\,^1\Sigma^+) \rightarrow NO^+(a\,^3\Sigma^+)$ and in the elastic scattering spectrum. Finally, resonances converging to the $NO^+(w\,^3\Delta)$ state interact with three continua, the previous two and $NO^+(b\,^3\Pi) + e^-$; they appear as resonances in each of the three continua. As will be seen below, the closeness of the various thresholds causes considerable overlap between the different Rydberg series.

As in the previous section, we study three total symmetries: $^2\Sigma^+$, $^2\Pi$ and $^2\Delta$. We also performed calculations for symmetry $^2\Phi$, but found that this symmetry has no significant contribution to the cross sections discussed in this work. The resonances series anticipated for each Rydberg limit are indicated in table 4. Note that because our continuum basis is restricted to functions of δ symmetry or less, Rydberg series with $\lambda \geqslant 3$ are not considered in this calculation.

Table 4. Series of resonances expected in a four-state scattering calculation. Rydberg limit in the first row and total system symmetry in the first column.

	$a\,^3\Sigma^+$	$b\,^3\Pi$	$w\,^3\Delta$
$^2\Sigma^+$	$s\sigma, p\sigma, \ldots$	$p\pi, d\pi, \ldots$	$d\delta, f\delta, \ldots$
$^2\Pi$	$p\pi, d\pi, \ldots$	$s\sigma, p\sigma, \ldots$ $d\delta, f\delta, \ldots$	$p\pi, d\pi, \ldots$
$^2\Delta$	$d\delta, f\delta, \ldots$	$p\pi, d\pi, \ldots$	$s\sigma, p\sigma, \ldots$

Analysis of electron-impact electronic excitation of ground-state NO^+ shows that the cross sections are dominated by these resonances. Their omission would lead to a serious underestimate of the excitation cross section.

Figure 2 shows the total cross section, summed over the three symmetries considered, for the electron-impact electronic excitation $NO^+(X\,^1\Sigma^+) \rightarrow NO^+(a\,^3\Sigma^+)$. The three ionization limits are indicated with vertical broken lines. It is hard to resolve the Rydberg structure of the resonances converging to the $b\,^3\Pi$ state because this state is too close to the $a\,^3\Sigma^+$ state. On the other hand, the $w\,^3\Delta$ Rydberg series is clearly above the $b\,^3\Pi$ threshold.

The total cross section for the transition $NO^+(X\,^1\Sigma^+) \rightarrow NO^+(b\,^3\Pi)$ is shown in figure 3. In this figure, the Rydberg series converging to the $w\,^3\Delta$ state is superimposed on a wide feature (peak at 7.87 eV) present in two-state calculations, and indeed simpler models not discussed here, with $^2\Delta$ symmetry. It seems likely that this structure comes from a resonance associated with a target state not explicitly included in our calculation.

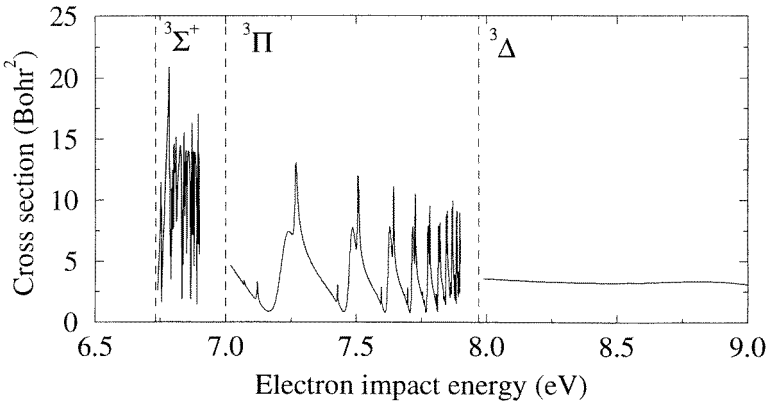

Figure 2. Total cross section of the electronic excitation $NO^+(X\,^1\Sigma^+) \rightarrow NO^+(a\,^3\Sigma^+)$ as a function of the electron-impact energy.

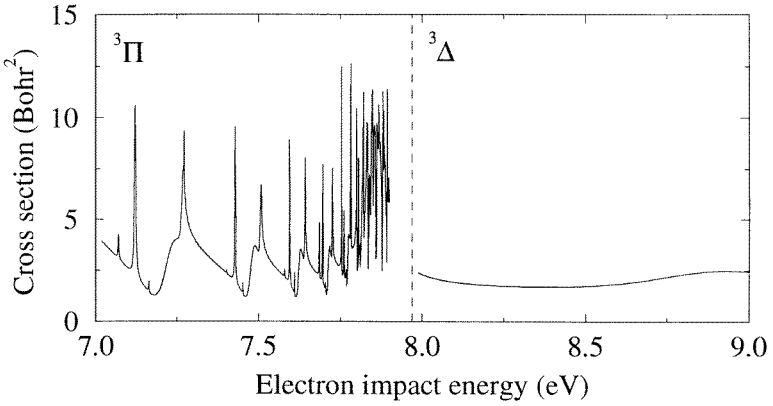

Figure 3. Total cross section of the electronic excitation $NO^+(X\,^1\Sigma^+) \rightarrow NO^+(b\,^3\Pi)$ as a function of the electron-impact energy.

To study the large number of resonances detected in the 0–10 eV energy range, we follow the work of Tennyson (1988) and use quantum defect theory (Seaton 1983, Moores and Saraph 1983) to classify and characterize the different Rydberg series detected.

The resonances were fitted to a Breit–Wigner profile to obtain their energy (E_r) and width (Γ) using the RESON program (Tennyson and Noble 1984). From these magnitudes, the complex quantum defects given by $\mu = \alpha + i\beta$, were obtained using the relations

$$E_r = E_t - \frac{1}{v_{nl\lambda}^2} \qquad \Gamma = \frac{2\beta}{v_{nl\lambda}^3} \tag{6}$$

where $v_{nl\lambda} = n - \alpha_{nl\lambda}$ and n is an integer. E_t is the energy of the threshold to which the Rydberg series converges with energies in Ryd.

In general, we find that the resonances are narrow. The broadest is the lowest $^2\Sigma^+$ resonance at 1.156 eV which is 70 meV wide. The only other resonance broader than ~ 10 meV is the lowest $^2\Pi$ state correlating with the b $^3\Pi$ state at 3.738 eV which is 39 meV wide. These resonances are sufficiently narrow that one would expect their vibrational

structure to be resolved in any direct measurement sensitive to them.

In the following subsections, we compare the results obtained in each one of the total symmetries considered in previously published work. All previous work appears to have focused entirely on resonance positions, as given by α, rather than widths, represented by β in tables 5–7.

Table 5. α and β parameters for the Rydberg resonances series of symmetry $^2\Sigma^+$. Numbers in brackets are powers of ten.

	a $^3\Sigma^+$							
n	sσ		pσ		dσ		fσ	
2			0.438	4.9(−3)				
3	1.027	1.3(−3)	0.644	9.9(−4)	−0.075	6.6(−4)		
4	1.119	9.9(−4)	0.612	1.4(−3)	−0.097	4.6(−4)		
5	1.103	8.2(−4)	0.600	1.2(−3)	−0.100	6.9(−4)	0.037	1.7(−3)
6	1.131	1.1(−3)	0.593	1.3(−3)	−0.105	5.6(−4)		
7			0.591	1.3(−3)	−0.108	1.2(−3)	0.069	4.0(−3)
8	1.142	9.6(−4)	0.578	1.8(−3)				
9	1.134	1.8(−3)						
10	1.125	3.1(−3)	0.586	1.2(−3)				
11	1.130	1.3(−3)	0.587	1.4(−3)	−0.094	5.1(−4)		
12	1.136	9.2(−4)	0.589	1.7(−3)	−0.070	6.7(−3)		
13	1.138	7.4(−3)			−0.085	2.1(−2)		
	b $^3\Pi$				w $^3\Delta$			
n	pπ		dπ		dδ		fδ	
3	0.594	1.2(−3)	−0.096	7.2(−4)	0.009	2.3(−3)		
4	0.637	1.3(−3)	−0.059	9.4(−4)	0.008	5.3(−3)	0.000	3.2(−4)
5	0.635	9.8(−4)	−0.076	1.4(−3)	0.011	5.3(−3)	0.000	1.0(−4)
6	0.632	1.2(−3)	−0.103	4.0(−2)	0.013	4.9(−3)	0.000	3.0(−4)
7					0.015	4.7(−3)	0.000	5.3(−4)
8	0.631	4.0(−3)	−0.100	2.4(−3)	0.016	4.3(−3)	0.000	1.0(−7)
9	0.630	4.0(−3)	−0.103	2.3(−3)	0.016	4.1(−3)	0.000	8.2(−4)
10	0.628	3.9(−3)	−0.105	2.3(−3)	0.017	4.0(−3)		
11	0.627	3.9(−3)	−0.106	2.3(−3)	0.015	4.4(−3)	−0.001	1.4(−3)
12	0.626	3.8(−3)			0.015	3.9(−3)		
13					0.020	4.2(−3)		

4.1. $^2\Sigma^+$ symmetry

In table 5, we present the parameters α and β for the series with total symmetry $^2\Sigma^+$. The table shows that not all the resonance series anticipated have actually been resolved given that we included six partial waves for each total symmetry. In the case of the a $^3\Sigma^+$ limit, three full series were obtained and two members of a higher series; just two series were resolved converging to the b $^3\Pi$ and w $^3\Delta$ limits.

The resonances of $^2\Sigma^+$ symmetry are particularly easy to assign. This is because the energy difference between the X $^1\Sigma^+$ and a $^3\Sigma^+$ thresholds is large and there are no s series converging to the b $^3\Pi$ state nor s and p to the w $^3\Delta$ state. This means that the Rydberg states associated with a $^3\Sigma^+$ appear almost unperturbed. Thus, we find few cases in which resonances overlap. However, there are interactions between the pairs: 5sσ–3dπ, 5fσ–4dπ and 7fσ–4dδ. We note that the coincidence between these members depends on the

Table 6. α and β parameters for the Rydberg resonances series of symmetry $^2\Pi$. Numbers in brackets are powers of ten.

	a $^3\Sigma^+$						w $^3\Delta$					
n	pπ		dπ		f, g?π		pπ		dπ		f, g?π	
2							0.096	1.5(−3)				
3	1.182	2.0(−3)	−0.057	5.2(−4)			0.624	9.2(−4)	0.070	7.6(−3)		
4	0.747	1.3(−3)	−0.058	2.4(−3)			0.611	1.2(−4)	−0.242	1.2(−1)	0.001	4.7(−4)
5	0.641	4.9(−3)	0.000	1.3(−2)			0.617	1.7(−2)	−0.247	1.0(−1)	−0.002	3.6(−3)
6	0.633	3.7(−3)			0.108	7.3(−2)	0.614	1.6(−2)	−0.227	7.7(−2)	0.006	3.8(−3)
7	0.633	1.1(−2)	−0.053	3.6(−3)	−0.125	5.1(−3)	0.613	1.6(−2)	−0.222	6.7(−2)	0.002	5.1(−4)
8	0.623	5.3(−3)					0.612	1.6(−2)	−0.220	6.6(−2)	0.003	3.4(−4)
9	0.634	4.8(−3)	−0.082	6.3(−4)			0.612	1.6(−2)	−0.218	6.2(−2)	0.022	1.7(−2)
10	0.642	3.1(−3)	−0.060	2.8(−3)			0.594	2.5(−2)			0.001	1.1(−3)
11	0.649	3.0(−3)	−0.055	2.0(−3)								
12			−0.041	1.9(−2)								
13	0.642	7.7(−3)	−0.058	8.5(−3)								

	b$^3\Pi$											
n	sσ		pσ		dσ		fσ		dσ		fσ	
3	0.959	6.1(−3)	0.640	1.2(−3)	−0.130	1.5(−3)			−0.018	5.7(−4)		
4	1.099	9.7(−4)	0.663	1.9(−3)	−0.165	3.8(−3)	0.041	8.1(−4)	−0.020	2.6(−5)	0.017	1.3(−3)
5	1.131	4.8(−3)	0.664	6.5(−3)	−0.167	6.3(−3)	0.032	2.2(−3)	−0.036	2.2(−3)	0.026	6.6(−4)
6	1.089	3.8(−4)	0.628	2.5(−3)	−0.143	2.9(−3)	0.033	1.5(−4)	−0.007	6.8(−4)	0.019	7.5(−5)
7	1.110	1.3(−3)										
8			0.641	1.9(−2)	−0.161	2.6(−2)	0.072	9.5(−4)	−0.001	1.2(−2)	0.004	9.1(−3)
9	1.133	3.3(−2)	0.629	2.0(−2)	−0.147	2.8(−2)	0.070	1.0(−3)	−0.008	9.0(−3)		
10			0.626	2.6(−2)	−0.150	3.3(−2)	0.073	4.3(−2)	−0.018	7.2(−2)		

relative energy of the thresholds and the internuclear separation chosen. This means that the interactions between these particular pairs may be an artefact of the parameters used in the present calculation. These interactions cause the irregularities seen in our quantum defects for these states. The rest of the states vary smoothly with n. This indicates that there are no interactions between them, or at least the interactions do not depend on near (accidental) degeneracies.

The experimental data of Erman *et al* (1995), Stubbs *et al* (1986) and Edqvist *et al* (1970) for $n = 3, 4, 5$ of the sσ series give $\alpha \sim 1.0$; there are no data for other σ series. Our results, with the exception of $\alpha_{3s\sigma}$, are about 0.1 higher. Swapping our sσ and dσ series, as discussed for the bound states, would give $\alpha_{s\sigma} \sim 0.9$ and $\alpha_{d\sigma} \sim 0.1$. In the absence of experimental data for $\alpha_{d\sigma}$, it is not possible for us to say which assignment is more appropriate for the observed data.

For the pπ series, the experimental results of Erman *et al*, Stubbs *et al* and Edqvist *et al* all give α in the range ∼0.70–0.77. The theoretical results of Stratmann *et al* (1996) and Hermann *et al* (1986) are both ∼0.62, very similar to our value of ∼0.63. This discrepancy between theory and experiments is similar to that found for bound Rydberg states of NO and could again be due to neglect of nuclear motion effects in all the calculations.

Stubbs *et al* (1986) also give results for dπ series. They obtained $\alpha \sim 0.002$. The theory of Hermann *et al* gave ∼0.10 and Stratmann *et al* ~ -0.129. Our results are close to this last one, with $\alpha_{d\pi} \sim -0.1$, which is in line with values obtained for bound states experimentally (e.g. Miescher and Huber 1964).

Table 7. α and β parameters for the Rydberg resonances series of symmetry $^2\Delta$. Numbers in brackets are powers of ten.

	a $^3\Sigma^+$		b $^3\Pi$					
n	d, fδ		pπ		dπ		f, g?π	
3	0.002	7.2(−4)	0.606	2.6(−4)	−0.102	1.2(−5)		
4	−0.007	1.5(−3)	0.638	1.3(−4)	−0.109	1.3(−4)	0.021	3.7(−2)
5	0.025	1.6(−4)	0.631	1.3(−3)	−0.102	1.3(−4)	0.007	5.0(−5)
	0.015	1.8(−3)						
6	−0.017	1.5(−3)	0.642	1.4(−4)	−0.107	1.3(−4)	0.006	4.6(−3)
7	0.019	1.0(−7)						
8	0.031	5.2(−4)	0.614	4.4(−3)	−0.144	1.8(−3)	0.090	2.0(−3)
9	0.006	5.9(−4)	0.613	4.3(−3)	−0.118	1.8(−3)	0.016	2.1(−3)
10	−0.005	1.8(−2)	0.613	4.2(−3)	−0.116	1.8(−3)	0.012	2.0(−4)
11	0.016	3.8(−3)	0.613	4.1(−3)	−0.115	1.8(−3)	0.007	1.0(−7)
12	0.026	3.8(−4)						
	w $^3\Delta$							
n	sσ		pσ		dσ		fσ	
3	1.042	1.4(−4)	0.658	2.3(−4)	−0.086	1.7(−5)		
4	1.113	5.4(−5)	0.608	5.1(−3)	−0.097	2.2(−3)	0.002	1.1(−3)
5	1.121	2.9(−3)	0.602	1.8(−3)	−0.104	2.0(−3)	0.000	1.8(−4)
6	1.127	2.5(−3)	0.597	2.0(−3)	−0.107	2.0(−3)	0.000	3.1(−4)
7	1.132	2.4(−3)	0.596	2.4(−3)	−0.109	2.1(−3)	0.001	4.4(−4)
8	1.138	3.0(−3)	0.596	3.4(−3)	−0.111	2.3(−3)	0.005	8.2(−4)
9	1.148	5.9(−3)						

4.2. $^2\Pi$ *symmetry*

The $^2\Pi$ resonances are far more complicated than those of $^2\Sigma^+$ symmetry since Rydberg series with all l converge to the b $^3\Pi$ threshold and there are two projections for the Rydberg electron angular momentum that generate σ and δ series. The low-l members of these series mix with each other and with the series converging to the a $^3\Sigma^+$ state.

Table 6 gives complex quantum defects for the series of resonances found below the three thresholds considered. The main interactions, in this case, are 6pπ(a $^3\Sigma^+$)–6fπ(a $^3\Sigma^+$)–3dπ(w $^3\Delta$) and 4fδ(b $^3\Pi$)–4dδ(b $^3\Pi$)–4fσ(b $^3\Pi$). The values of quantum defects are similar to those obtained for the $^2\Sigma^+$ symmetry. The main difference to note is the relatively large negative value, -0.2, for the dπ series converging to the w $^3\Delta$ state and the small value, -0.05, of the dπ series converging to the a $^3\Sigma^+$ state.

In this case, our value for $\alpha_{3s\sigma} \sim 0.96$ agrees surprisingly well with that of Stratmann *et al* (0.96) and Stubbs *et al* (~ 1.01). Hermann *et al* give values for this series for $n = 3, 4$ and 5 which start with $\sim$0.98 and decrease as n increases. We find the reverse trend: our values increase from 0.96 to ~ 1.13 for $n = 5$.

To find a possible cause of this discrepancy, we should look at the dσ series. In this case, our α values are ~ -0.15 while Stubbs *et al* give ~ 0.15 and Hermann *et al* ~ 0.09. Swapping the sσ and dσ series, gives $\alpha_{s\sigma} \sim 1.15$, $\alpha_{d\sigma} \sim 0.01$ for the data of Stubbs *et al* and $\alpha_{s\sigma} \sim 1.09$, $\alpha_{d\sigma} \sim -0.02$ for the data of of Hermann *et al*. This is closer to our values in each case. This possible swap of the series assignments is the same as that proposed for the Rydberg states discussed in section 3. In that case we based our assignments on the character of the wavefunctions above threshold and found agreement with the works of

Fredin *et al* (1987), Miescher and Huber (1976) and Kaufmann (1991).

For the pσ series, experimental and theoretical values are in the range ~ 0.65–0.70 (with $n = 3$–5). Our results are in the lower part of this range for these values of n.

4.3. $^2\Delta$ *symmetry*

In this case, the sσ and pσ series are not present in the Rydberg series leading to the a $^3\Sigma^+$ state. This greatly reduces the number of mixed resonances. Table 7 gives the quantum defects calculated for the resonances of symmetry $^2\Delta$. These results are similar to those presented for symmetries $^2\Sigma^+$ and $^2\Pi$.

For the pπ series, our α values are 0.61–0.63 compared with those of Hermann *et al* (0.68–0.65) and Stratmann *et al* (0.7). Experimental values are the same as those presented for the $^2\Sigma^+$ symmetry.

For the dπ series, the value of Stratmann *et al*, $\alpha_{3d\pi} = -0.042$ is closer to our value of -0.1 than the value, 0.06, of Hermann *et al* and the experimental value of 0.002 of Stubbs *et al*, seen in $^2\Sigma^+$ symmetry. In this case, the discrepancy with Stubbs *et al* and Hermann *et al* cannot be explained by swapping s and d series, since there is no sπ series.

Hermann *et al* give one value for the series fπ: $\alpha_{4f\pi} = 0.01$, which is close to our value of 0.02.

For the sσ series, the experimental values of Erman *et al*, Stubbs *et al* and Edqvist *et al* are concentrated around $\alpha_{s\sigma} \sim 1.0$, while our values are around ~ 1.1. For the dσ series, the values of Stubbs are ~ 0.1, while ours are ~ -0.1. Here again swapping the experimental assignments removes this discrepancy.

Finally, Stubbs *et al* found $\alpha \sim 0.7$ for the pσ series, somewhat higher than our value of ~ 0.6.

5. Conclusions

We have studied the Rydberg bound states of the NO molecule and its continuum states using the molecular R-matrix method. We employed CI wavefunctions to represent the NO^+ ion and close-coupling models including either two or four NO^+ target states. Three total symmetries, $^2\Sigma^+$, $^2\Pi$ and $^2\Delta$, were considered enough to obtain convergence in cross sections for the electron-impact electronic excitation $NO^+(X\ ^1\Sigma^+) \rightarrow NO^+(a\ ^3\Sigma^+, b\ ^3\Pi)$.

Quantum defect theory was used to classify the large number of bound states and resonances obtained. For the bound states, we find that most of the Rydberg series follow a linear correlation between their quantum defects and the energy of the Rydberg electron and, at $n = \infty$, we find a surprisingly large p–d mixing. For resonances, we give comprehensive data on Rydberg series converging to the thresholds a $^3\Sigma^+$, b $^3\Pi$ and w $^3\Delta$. We obtain satisfactory agreement between our calculations and data available. The exception is for the d series, which appear shifted to higher energies than seems to be found experimentally. We present the first data on the resonance widths.

Finally, this work is limited to a single NO bond length and a target description of four states that were obtained with a reduced active space in which six electrons were kept in frozen orbital and eight (nine) electrons were allow to occupied three σ and two π orbitals in the molecular ion (scattering) system. This produces a limited treatment of correlation effects of the target and between the Rydberg electron and the ion, effects that have been shown to be important for an accurate treatment of the penetrating s, p and d series Rydberg electron (Kaufmann 1991). This could be responsible for the small systematic deviation

found in s, p and d series. We are in a position to improve this description in future calculations by using the new code SCATCI (Tennyson 1996). This will allow for both the enlargement of the active space (improving correlation effects) and the number of CI states in the target close-coupling expansion. This and the effects of varying the NO internuclear separation will be the subject of future work.

Acknowledgments

We thank Lesley Morgan for many helpful discussions, Susan Branchett for help with the initial calculations and Charles Gillan for providing orbitals for test calculations. This work was supported by the UK Engineering and Physical Sciences Research Council under grant GR/K47702 and the National Science Foundation through a grant for the Institute for Theoretical Atomic and Molecular Physics at Harvard University and Smithsonian Astrophysical Observatory.

References

Albritton D L, Schmeltekopf A L and Zare R N 1979 *J. Chem. Phys.* **71** 3271
Billingsley F P II 1975 *J. Chem. Phys.* **3** 864
Edlén B 1964 *Handbuch der Physik* vol 27 (Berlin: Springer)
Edqvist O, Lindholm E, Selin L E, Sjögren H and Åsbrink L 1970 *Ark. Fys.* **40** 439
Erman P, Karawajczyk A, Rachelew-Källne E and Strömholm C 1995 *J. Chem. Phys.* **102** 3064
Errea L F, Harel C, Jouin H, Méndez L, Pons B and Riera A 1994 *J. Phys. B: At. Mol. Opt. Phys.* **27** 3603
Fehér M and Martin P A 1993 *Chem. Phys. Lett.* **215** 565
Fredin S, Gauyacq D, Horani M, Jungen C, Lefevre G and Masnou-Seeuws F 1987 *Mol. Phys.* **60** 825
Fujii A, Ebata T and Ito M 1990 *J. Chem. Phys.* **90** 6993
Gillan C J, Tennyson J and Burke P G 1995 *Computational Methods for Electron–Molecule Collisions* ed W M Huo and F A Gianturco (New York: Plenum)
Gilmore F R 1965 *J. Quant. Spectrosc. Radiat. Transfer* **5** 369
Guo J, Mank A and Hepburn J W 1995 *Phys. Rev. Lett.* **74** 3584
Hermann M R, Bauschlicher C W Jr, Huo W M and Langhoff S R 1986 *Chem. Phys.* **109** 1
Huber K P and Herzberg G 1979 *Molecular Spectra and Molecular Structure* vol 4 *Constants of Diatomic Molecules* (New York: Van Nostrand-Reinhold)
Huo W M and Gianturco F A (eds) 1995 *Computational Methods for Electron–Molecule Collisions* (New York: Plenum)
Jastrow R 1948 *Phys. Rev.* **73** 60
Kaufmann K 1991 *J. Phys. B: At. Mol. Opt. Phys.* **24** 2277
Lindholm E 1970 *Ark. Fys.* **40** 97
Liu L and Li J-M 1991 *J. Phys. B: At. Mol. Opt. Phys.* **24** 1893
Miescher E 1976 *Can. J. Phys.* **54** 2074
Miescher E and Huber K P 1964 *International Review of Science* vol 3 *(Physical Chemistry Series Two)* (London: Butterworth)
Moores D L and Saraph H E 1983 *Atoms in Astrophysics* (New York: Plenum)
Morgan L A 1984 *Comput. Phys. Commun.* **31** 419
Noble C J and Nesbet R K 1984 *Comput. Phys. Commun.* **33** 399
Park H, Leahy D J and Zare R N 1996 *Phys. Rev. Lett.* **76** 1591
Partridge H, Langhoff S R and Bauschlicher Jr C W 1990 *J. Chem. Phys.* **93** 7179
Sarpal B K, Branchett S E, Tennyson J and Morgan L A 1991 *J. Phys. B: At. Mol. Opt. Phys.* **24** 3685
Seaton M J 1983 *Rep. Prog. Phys.* **46** 167
Stratmann R E, Zurales R W and Lucchese R R 1996 *J. Chem. Phys.* **104** 8989
Stubbs R J, York T A and Comer J 1986 *Chem. Phys.* **106** 161
Tennyson J 1988 *J. Phys. B: At. Mol. Opt. Phys.* **21** 805
——1996 *J. Phys. B: At. Mol. Opt. Phys.* **29** 1817
Tennyson J and Noble C J 1984 *Comput. Phys. Commun.* **33** 421

Tennyson J, Noble C J and Salvini S 1984 *J. Phys. B: At. Mol. Phys.* **17** 905
Vrakking M J J and Lee Y T 1995 *J. Chem. Phys.* **102** 8818
Wayne R P 1991 *Chemistry of Atmospheres* 2nd edn (Oxford: Clarendon)